

Medical Image Analysis



॥ त्वं ज्ञानमयो विज्ञानमयोऽसि ॥

Angshuman Paul

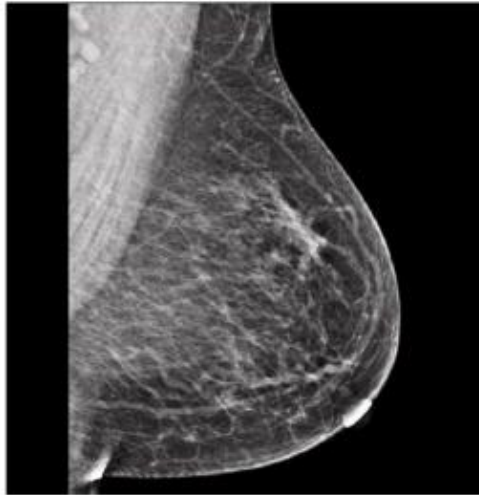
Assistant Professor

Department of Computer Science & Engineering

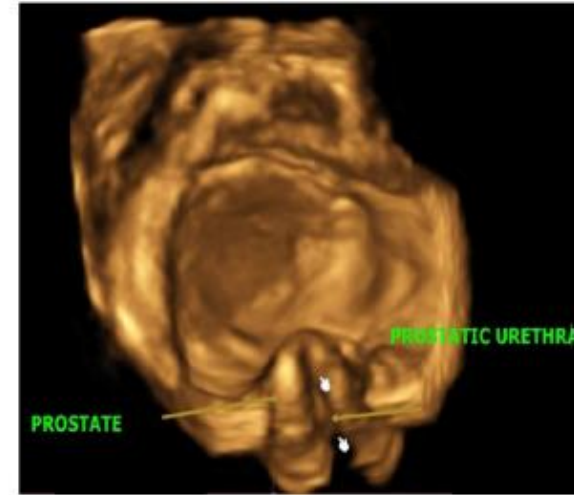
Ultrasound Images



(a) A fetus US image.



(b) A breast US image.



(c) A 3D prostate US image.

Fig. 1. Three examples of US images of different organs (a 2D fetus, a 2D breast, and a 3D prostate).

Noise Removal

Noise in Ultrasound Images

- Speckle noise
 - Multiplicative
 - $I(x, y) = F(x, y)N(x, y)$

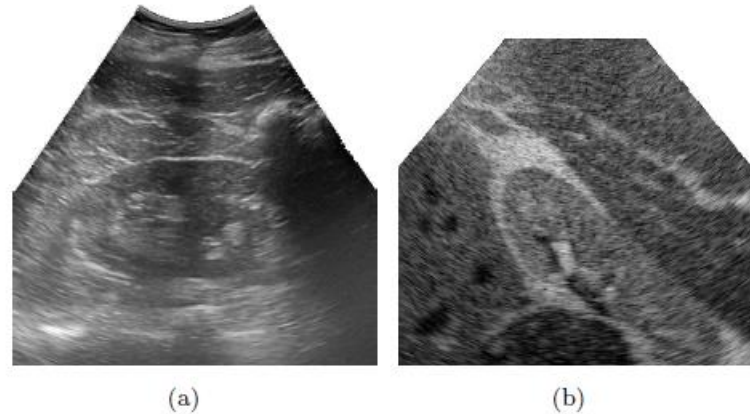
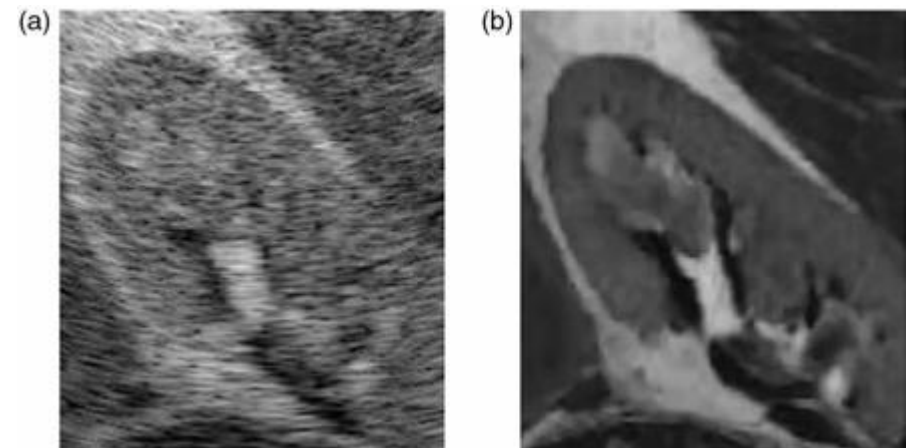


Figure 1. Speckle noise. (a) Real ultrasound image. (b) Simulated ultrasound image.

- May hide important information
- Can also provide meaningful information about anatomy



Lee Filter

$$k_s = 1 - C_u^2 / C_s^2.$$

$$\hat{I}_s = \bar{I}_s + k_s (I_s - \bar{I}_s)$$

Here,

$$C_s^2 = (1/|\eta_s|) \sum_{p \in \eta} (I_p - \bar{I}_s)^2 / (I_p - \bar{I}_s)^2$$

$$C_u^2 = 1/ENL$$

or

$$C_u^2 = \frac{\text{var}(z')}{(\bar{z}')^2}$$

- Designed to eliminate speckle noise while preserving edges and point features. Based on a linear speckle noise model.

Can Anisotropic Diffusion Remove Speckle?

$$\begin{cases} \frac{\partial I}{\partial t} = \operatorname{div}[c(|\nabla I|) \cdot \nabla I] \\ I(t=0) = I_0 \end{cases}$$

and

$$c(x) = \frac{1}{1 + (x/k)^2}$$

$$c(x) = \exp[-(x/k)^2]$$

Can Anisotropic Diffusion Remove Speckle?

$$\begin{cases} \frac{\partial I}{\partial t} = \operatorname{div}[c(|\nabla I|) \cdot \nabla I] \\ I(t=0) = I_0 \end{cases}$$

and

$$c(x) = \frac{1}{1 + (x/k)^2}$$

$$c(x) = \exp[-(x/k)^2]$$

AD will enhance speckle

Speckle Reducing Anisotropic Diffusion

$$I_{i,j}^{t+\Delta t} = I_{i,j}^t + \frac{\Delta t}{|\bar{\eta}_s|} \operatorname{div}[c(C_{i,j}^t) \nabla I_{i,j}^t]$$

Speckle Reducing Anisotropic Diffusion

$$\begin{cases} \partial I(x, y; t)/\partial t = \text{div}[c(q)\nabla I(x, y; t)] \\ I(x, y; 0) = I_0(x, y), (\partial I(x, y; t)/\partial \vec{n})|_{\partial\Omega} = 0 \end{cases}$$

$$c(q) = \exp\{-[q^2(x, y; t) - q_0^2(t)]/[q_0^2(t)(1 + q_0^2(t))]\}.$$

$$q(x, y; t) = \sqrt{\frac{(1/2)(|\nabla I|/I)^2 - (1/4^2)(\nabla^2 I/I)^2}{[1 + (1/4)(\nabla^2 I/I)]^2}}$$

$$q_0(t) = \frac{\sqrt{\text{var}[z(t)]}}{z(t)}$$

Speckle Reducing Anisotropic Diffusion

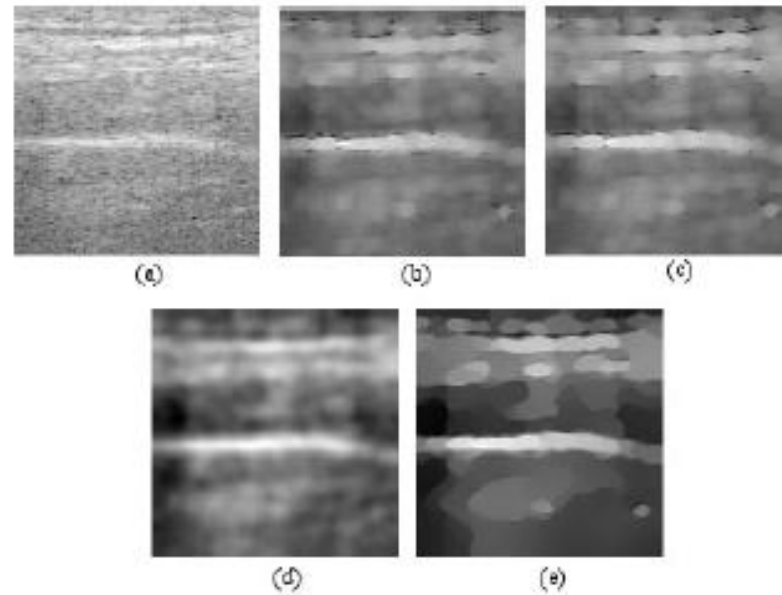


Fig. 4. (a) Original noisy image. (b)–(e) Filtered images from En-Lee, En-Frost, AD-Homomorph, and SRAD.

Shape Based Speckle Removal for Segmentation

$$\begin{aligned}
 & \sum_{p \in I} (I - I_O)^2 + \sum_i (r_i - \mu_r)^2 \\
 & - \sum_{p \in e(C_i)} (|\Delta I|)^2, \#|\Delta I|^2 > 0 \leq k.
 \end{aligned}$$

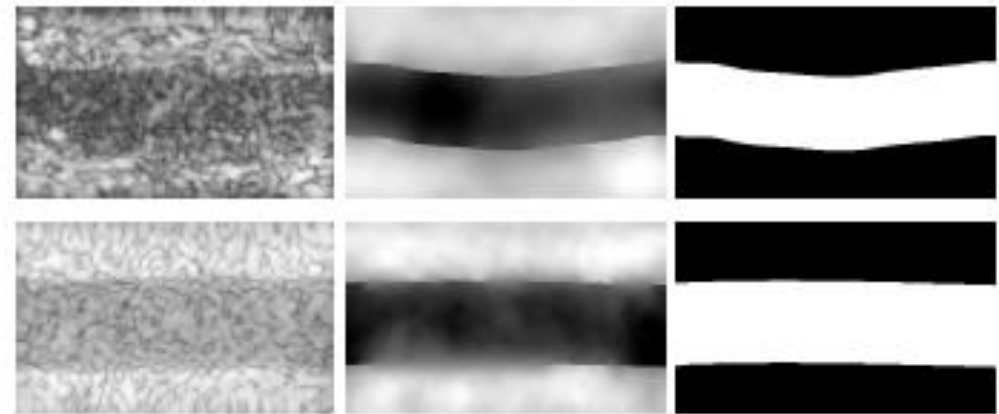


Fig. 1: Noise removal and segmentation (using [13]) in real (row 1) and phantom (row 2) datasets. Column 1: original image, column 2 and 3: speckle removal and segmentation (respectively) using the proposed method.

Speckle Reduction using Diffusion Potential

$$G^t(x, y) = \sum_{k=1}^K |V(L^t(x, y)) - V(L^t(x_k, y_k))| \hat{e}_k.$$

Gradient of
Local Variance

$$\psi^t(x, y) = V(L^t(x, y)) + |G^t(x, y)|.$$

Diffusion
Potential

$$D^t(x, y) = \exp \{ -\kappa t |\psi^t(x, y) - \xi^t(x, y)| \} ,$$

Diffusion
Coefficient

Speckle Reduction using Diffusion Potential

$$G^t(x, y) = \sum_{k=1}^K |V(L^t(x, y)) - V(L^t(x_k, y_k))| \hat{e}_k.$$

Gradient of Local
Variance

$$\psi^t(x, y) = V(L^t(x, y)) + |G^t(x, y)|.$$

Diffusion
Potential

$$D^t(x, y) = \exp \{ -\kappa t |\psi^t(x, y) - \xi^t(x, y)| \},$$

Diffusion
Coefficient

$$\xi^t(x, y) = \frac{\sum_{k=1}^K \psi^t(x_k, y_k) + \psi^t(x, y)}{K + 1}.$$

$$I_i^{t+1}(x, y) = I_i^t(x, y) - \lambda_i^t(x, y)(I_i^t(x, y) - \mu_\psi^t(x, y));$$

$$i \in \{v, b\}. \quad (5)$$

$$\lambda_i^t(x, y) = \beta D^t(x, y); \quad i \in \{v, b, e\}.$$

Speckle Reduction using Diffusion Potential

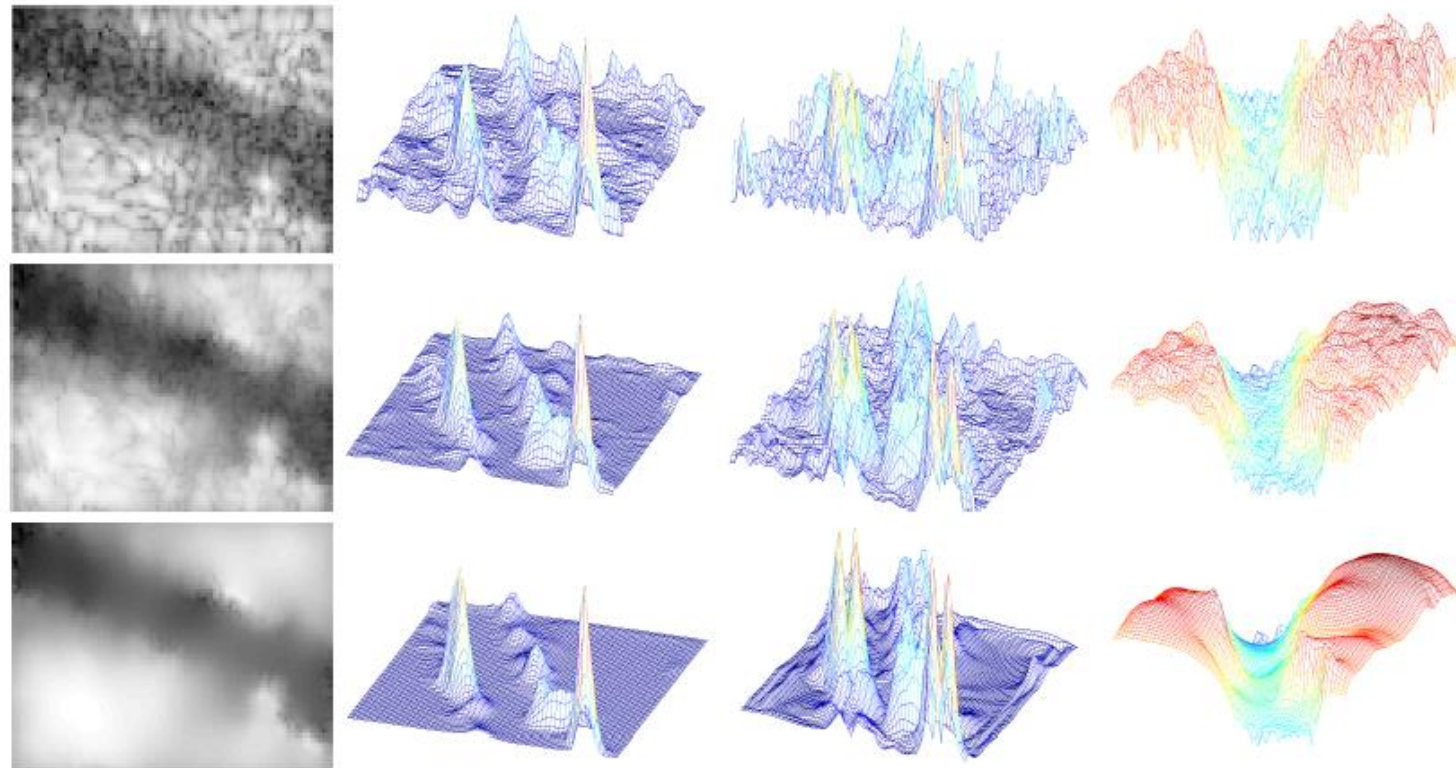


Fig. 1. Effect of iteration (in the rows) on an example image [21] during speckle removal: row 1: original image, row 2: 10 iterations, row 3: 50 iterations. Column 1: original image, column 2: local variance, column 3: gradient of local variance and column 4: intensity values.

Speckle Reduction using Diffusion Potential

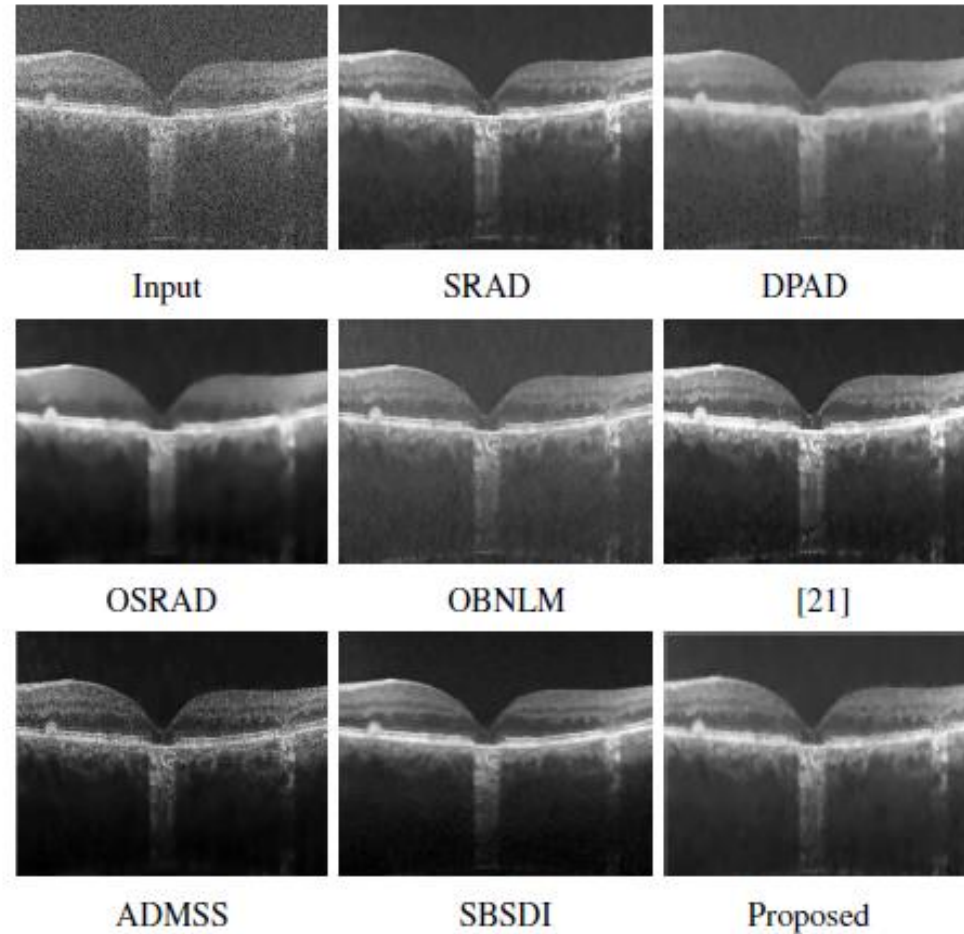


Fig. 3. Performances of different speckle removal methods on an example SDOCT image. Speckle artifacts are revealed clearly when the images are zoomed.

Motion Artifacts

- Most prominently visible in organs with motion (such as heart, circulatory organ)

Diagnosis of Breast Tumors: Multibranch U-Net

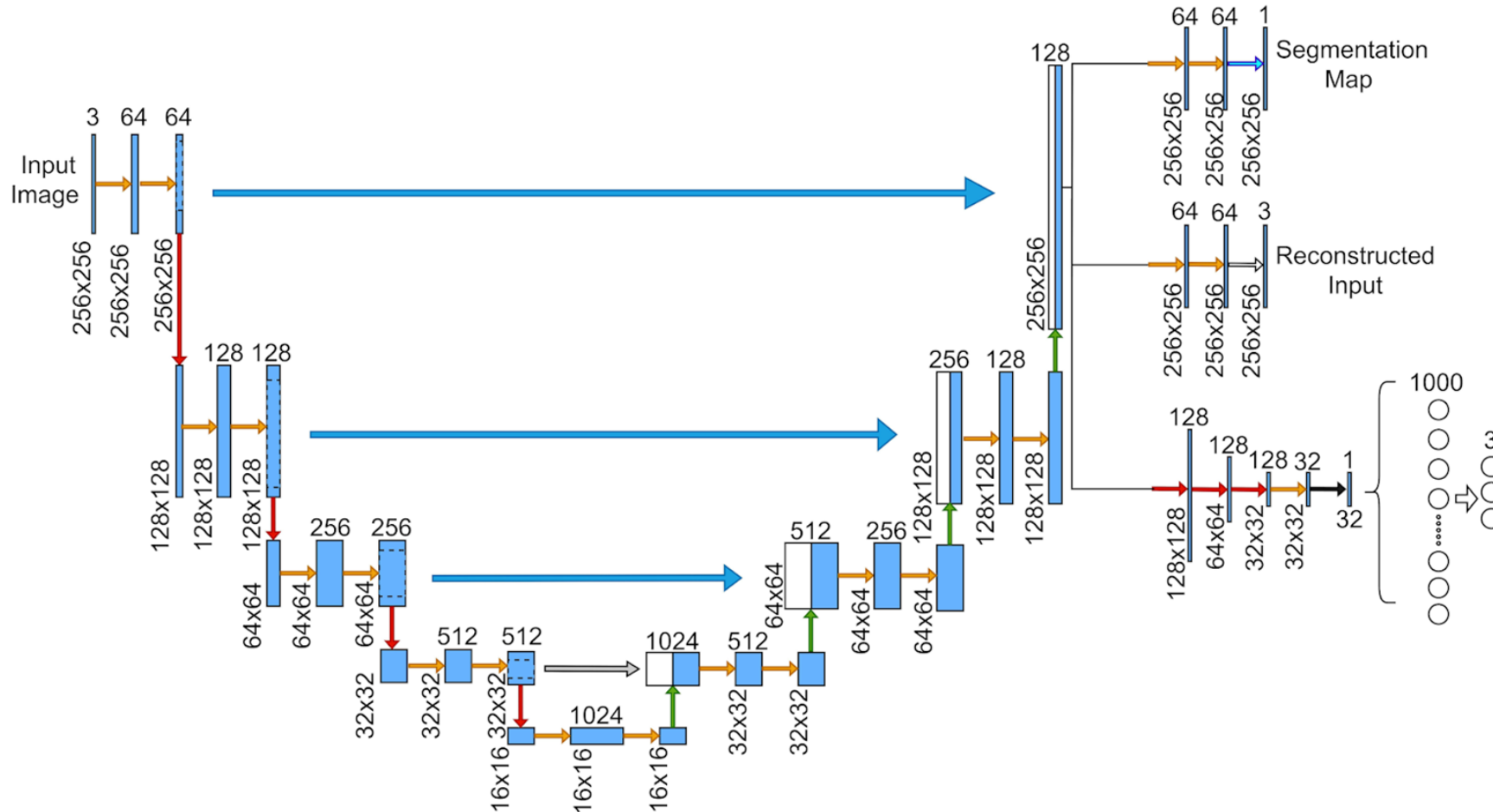
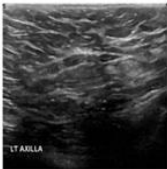

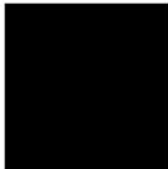






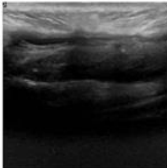

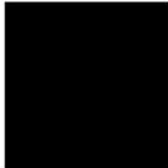

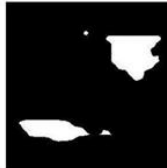




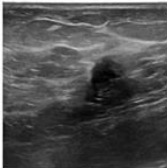
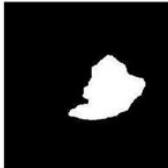
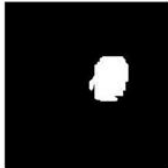






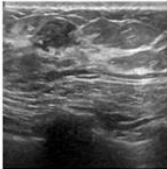

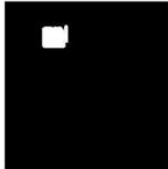

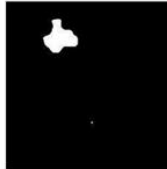




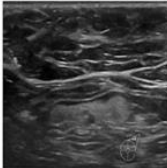

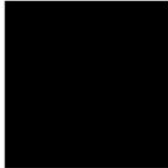






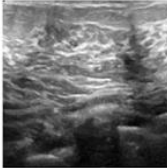

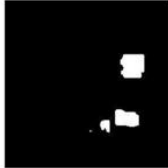


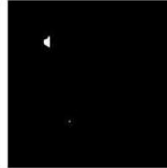





Image Type	Ultrasound Image	Ground Truth	Inception UNet	Attention UNet	PSPNet	UNet++	Residual UNet	UNet	Proposed
Benign									
Benign									
Malignant									
Malignant									
Normal									
Normal									

Diagnosis of Thyroid Nodules

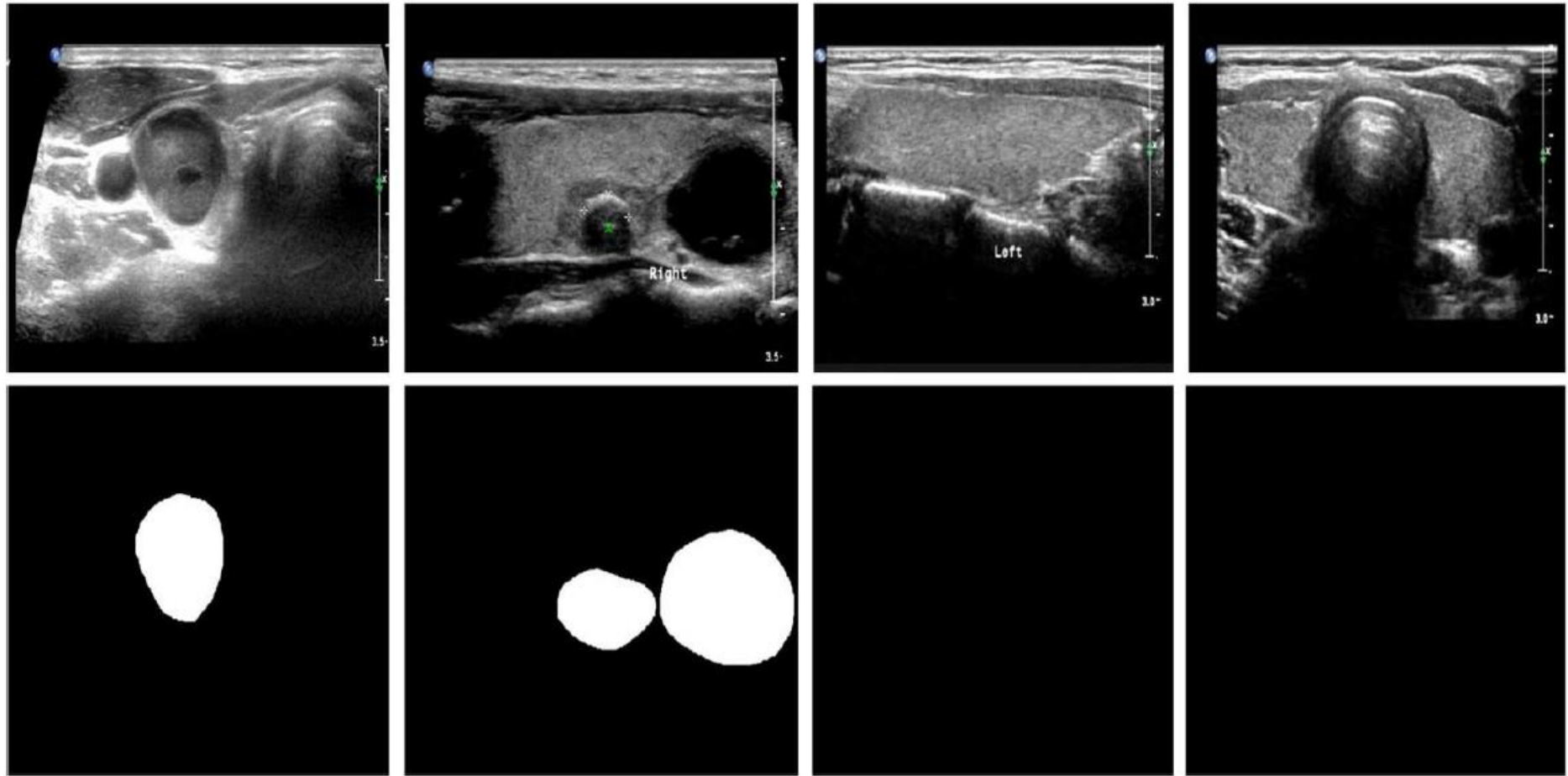


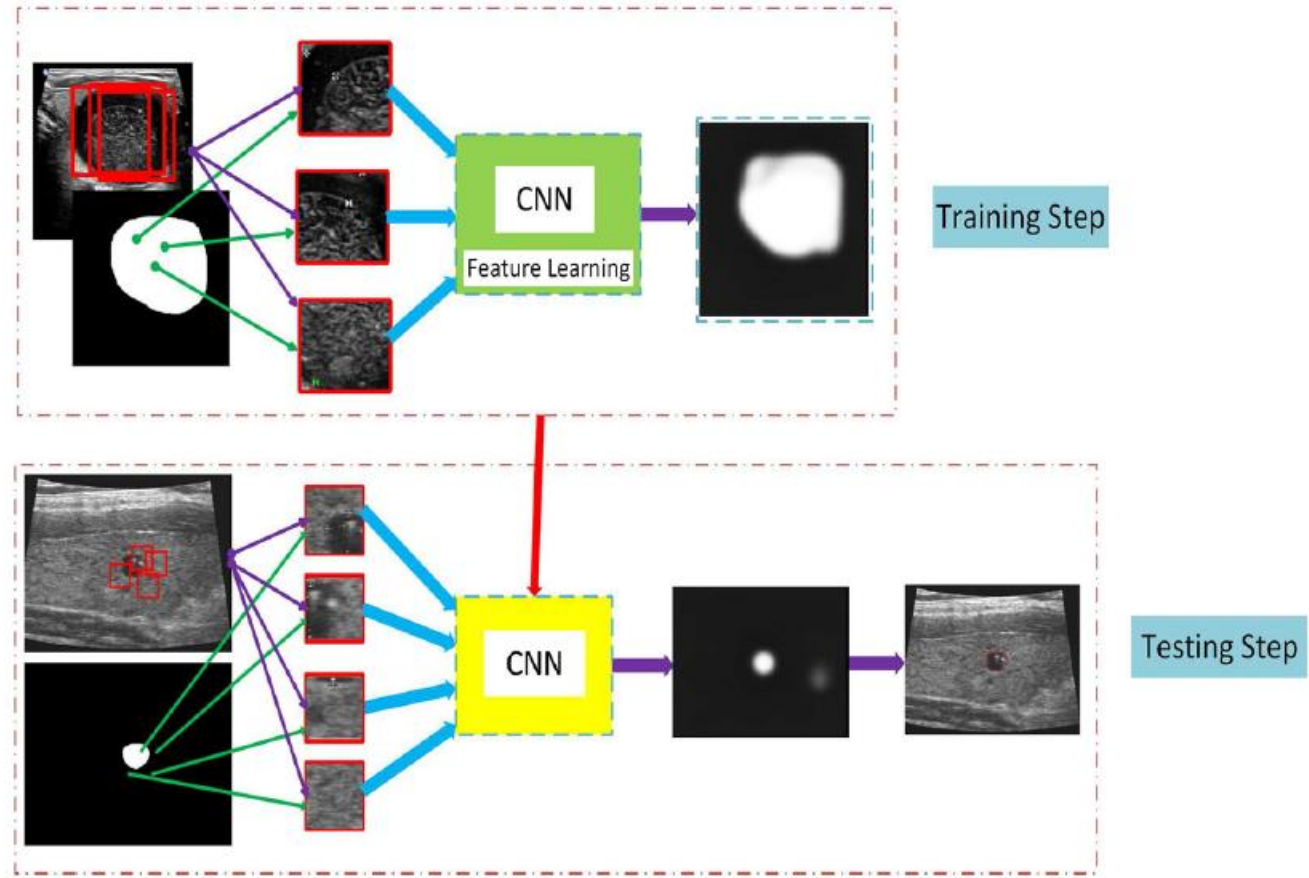
Fig. 2 Typical subimages of thyroid nodule(s) and normal thyroid (*top*), and the corresponding binary masks (*bottom*) used for training the CNN

Diagnosis of Thyroid Nodules

- TIRAD
- US guided FNAC

Diagnosis of Thyroid Nodules

Fig. 3 An framework of our CNN-based approach, which first extracts multiple nodule patches to capture the wide range of nodule variability from input 2D ultrasound images. The obtained patches are then fed into the networks simultaneously to compute discriminative features. Finally, our CNN-based approach applies a classifier to generate segmentation probability maps



Diagnosis of Thyroid Nodules: US Elasticity Imaging

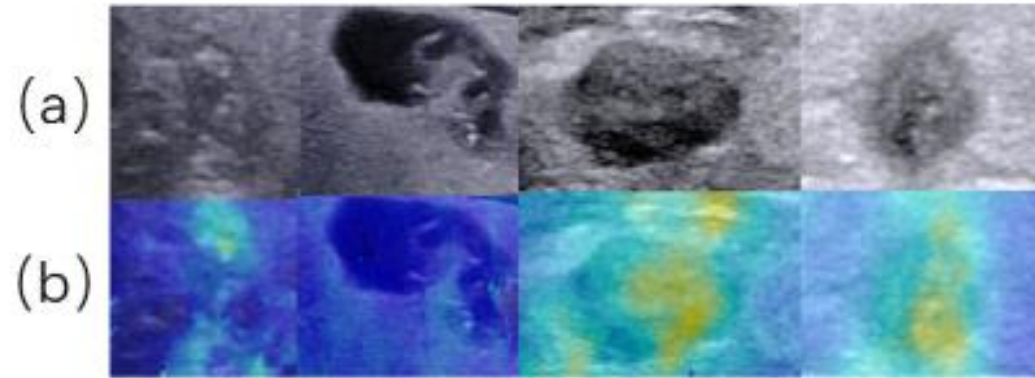


Fig. 2. Conventional ultrasound versus ultrasound elasticity imaging, (a) Conventional ultrasound nodule images, (b) Ultrasound elasticity nodule images. Both correspond to the extract same position.

Diagnosis of Thyroid Nodules: US Elasticity Imaging

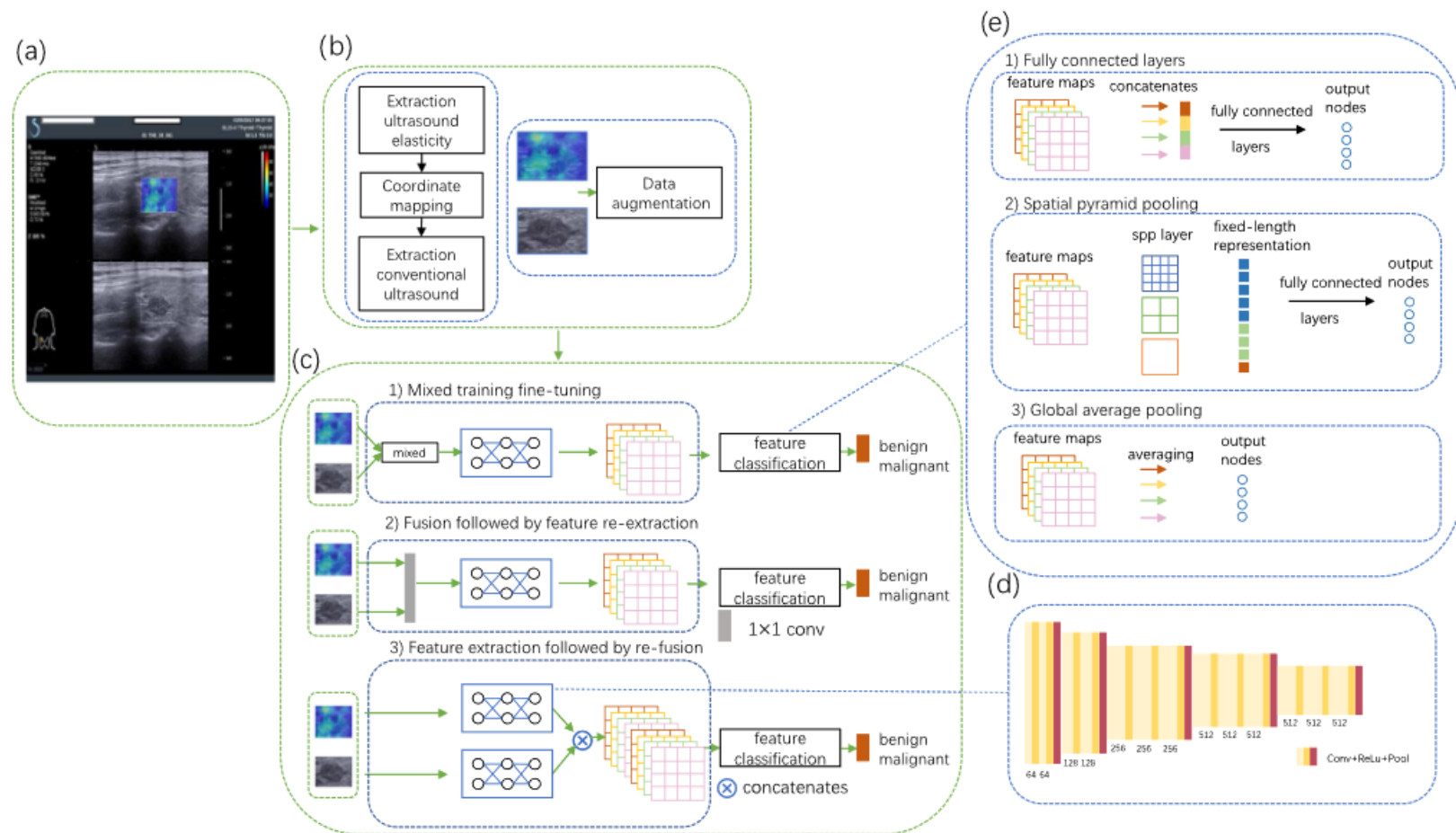


Fig. 4. Overview of the proposed method. (a) Raw input data. (b) Data preprocessing and data augmentation. (c) Fusion methods for two types of data. Orange boxes represent the nodule classification output. (d) Basic network architecture (VGG16). (e) Feature classification methods.